

Superimposed training low probability of detection underwater communications

Fabio B. Louza, and Harry A. DeFerrari

Citation: *The Journal of the Acoustical Society of America* **148**, EL273 (2020); doi: 10.1121/10.0001934

View online: <https://doi.org/10.1121/10.0001934>

View Table of Contents: <https://asa.scitation.org/toc/jas/148/3>

Published by the [Acoustical Society of America](#)

ARTICLES YOU MAY BE INTERESTED IN

[Sound field synthesis of arbitrary moving sources using spectral division method](#)

The Journal of the Acoustical Society of America **148**, EL247 (2020); <https://doi.org/10.1121/10.0001944>

[Transfer learning for efficient classification of grouper sound](#)

The Journal of the Acoustical Society of America **148**, EL260 (2020); <https://doi.org/10.1121/10.0001943>

[Rapid adaptation to non-native speech is impaired in cochlear implant users](#)

The Journal of the Acoustical Society of America **148**, EL267 (2020); <https://doi.org/10.1121/10.0001941>

[Machine learning in acoustics: Theory and applications](#)

The Journal of the Acoustical Society of America **146**, 3590 (2019); <https://doi.org/10.1121/1.5133944>

[Underwater sound generated by motor vehicle traffic in an underwater tunnel](#)

The Journal of the Acoustical Society of America **148**, EL215 (2020); <https://doi.org/10.1121/10.0001805>

[An experimental device for multi-directional somatosensory perturbation and its evaluation in a pilot psychophysical experiment](#)

The Journal of the Acoustical Society of America **148**, EL279 (2020); <https://doi.org/10.1121/10.0001942>



CALL FOR PAPERS

JASA
THE JOURNAL OF THE
ACOUSTICAL SOCIETY OF AMERICA

Special Issue:
Lung Ultrasound

The banner features a blue background with a grid pattern and a blurred image of an ultrasound probe. The text is in white and yellow.

Superimposed training low probability of detection underwater communications

Fabio B. Louza^{1,a)} and Harry A. DeFerrari²

¹Laboratory of Robotics and Engineering Systems (LARSys), University of Algarve, Campus de Gambelas, 8005-139, Faro, Portugal

²Rosenstiel School of Marine and Atmospheric Science, University of Miami, 4600 Rickenbacker Causeway, Miami, Florida 33149, USA
fblouza@ualg.pt, hdeferrari@rsmas.miami.edu

Abstract: This paper proposes a superimposed training method for low probability of detection underwater acoustic communications. A long pilot sequence was superimposed to the message for equalization and synchronization purposes. A fast Hadamard transform (FHT) estimated the channel impulse response and compressed the pilot energy. A Wiener filter performed equalization. The interference signal was removed using hyperslice cancellation by coordinate zeroing. An inverse FHT decompressed the remaining sequence energy and the message was retrieved. Results from a shallow water experiment presented bit error rates $< 10^{-2}$ for signal-to-noise ratios < -8 dB. © 2020 Acoustical Society of America.
<https://doi.org/10.1121/10.0001934>

[Editor: Paul Gendron]

Pages: EL273–EL278

Received: 15 May 2020 Accepted: 24 August 2020 Published Online: 17 September 2020

1. Introduction

In recent years, research on covert or low probability of detection (LPD)^{1,2} underwater acoustic communications has increased due to their several applications. In military applications, they have the potential to keep submarines and autonomous underwater vehicles (AUV) undetected while communicating to other submarines, surface vessels, or underwater network nodes.¹ Covert communications also have civilian applications including environmental monitoring telemetry, underwater sensor networking, and command and control of AUVs. The probability of detection depends on the signal-to-noise ratio (SNR) at the receiver, increasing for closer interceptors if emitted power is kept constant. Assuming that the unintended listener does not have previous knowledge about the signal, detection of the low SNR signals relies on an energy detector. Therefore, from several methods to measure the LPD capability of the system,¹ an arbitrary threshold of SNR at the receiver below -8 dB (Ref. 3) within the signal band has been chosen. There are several techniques used in LPD communications, but most common state-of-the-art systems use direct sequence spread spectrum (DSSS)^{1,2,4} signaling. DSSS uses a pseudo-random sequence (m-sequence) to spread data symbols bandwidth at the transmitter and a matched filter at the receiver to retrieve the data. Therefore, DSSS explores both the noise-like characteristics and the good correlation properties of m-sequences to avoid detection and to increase the processing gain of low power level signals.¹ However, DSSS requires precise symbol synchronization and tracking, hard to achieve at low SNR, and longer code sequences to minimize intersymbol interference, reducing the data rate.²

The objectives of this paper are to present a superimposed training method for underwater acoustic communications in a low SNR environment, and to demonstrate its feasibility for LPD communications based on a shallow water experiment. Superimposed training techniques present some benefits. First, no additional time slot is needed for the pilot or extra bandwidth consumption to estimate the channel impulse response (CIR). Second, there is no loss in the data rate and no data frequency spreading.⁵ Computationally simple, the proposed algorithm was developed to work with a fixed single low power source and a receiver, without an array gain. Before transmission, a bitstream is created superimposing a long training sequence to the message. Using a low power source, the bitstream is transmitted and repeated several times to permit the receiver to increase the processing gain and to implement error correction through coherent averaging. A Wiener filter⁶ performs equalization. A fast Hadamard transform (FHT)^{4,7,8} estimates the CIR and compresses the pilot energy. Performing efficient cyclic cross-correlation,

^{a)} Author to whom correspondence should be addressed.

FHT has found applications in both underwater digital communications⁴ and sonar data compression.⁹ After synchronization and averaging of the filtered bitstreams, a process called hyper-slice cancellation by coordinate zeroing (HCC0)^{4,8,9} removes the intentional interference. An inverse FHT over the remaining sequence decompresses the data energy and the message is retrieved. A shallow water experiment was performed in the bay of Arraial do Cabo on the coast of Rio de Janeiro/Brazil. Achieved bit error rates (BER) show that the approach is consistent. Compared to LPD benchmark³ (SNR < -8 dB), the results indicated the method's suitability for covert communications.

2. Superimposed training LPD method

The proposed method is divided in several steps, according to block diagram in Fig. 1.

2.1 Transmitted bitstream

A baseband bitstream is created superimposing a training sequence to the message symbol-by-symbol. Both sequences are binary phase-shift keying (BPSK) modulated of the same length. The pilot chip and data symbol rates are the same. Pseudo-random sequences, also called m-sequences, have useful properties for covert communications such as a noise-like characteristic and an impulse-like autocorrelation.^{4,7} Thus, a long m-sequence of length (L) 2047 bits (mseq2047) is used as the pilot code. In contrast to other superimposed training algorithms,⁵ the power of the pilot is slightly higher than the power of the message. In a low SNR environment, a stronger pilot can disguise the message in the background noise and yield a high pulse compression gain² for channel estimation, synchronization, and equalization. The message is composed of four consecutive streams of 511 bits. Each stream has a short m-sequence of 31 bits (mseq31), used later for hard synchronization, preceding a 480-bit data packet. The last three bits of the message do not carry information. Thus, the bitstream is created using mseq2047 code values ($c = \pm 1$) to modulate the carrier wave phase as given by [Eq. (1)]

$$s(t) = A \cos(2\pi f_c t + c\theta), \tag{1}$$

where A is the sum of the pilot and the message amplitudes, f_c is the carrier frequency, and $\theta = \pi/2$ (BPSK). In this work, the pilot to data amplitude ratio is 5/4 and each bit period contains four cycles of the carrier wave, sampled four times f_c .

2.2 Channel equalization and soft synchronization

The same bitstream of period T and k samples is transmitted and repeated Z times to increase the processing gain and to perform error correction through coherent averaging. A Wiener inverse filter⁶ is applied over each received sequence $y_Z(t + ZT)$ to mitigate multipath and reduce intersymbol interference. Using a replica of the known pilot code $x(k)$, the filter performs the channel equalization, estimating $g_Z(k)$. The soft synchronization of the filtered bitstreams $g_Z(k)$ involves several CIR $h_Z(k)$ estimations. Thus, an efficient FHT, also called fast M-sequence transform,⁷ is used to estimate $h_Z(k)$ from $g_Z(k)$. Taking advantage of the similarity between Hadamard matrices and m-sequences, the number of correlation operations can be reduced saving computational time. The reference for synchronization is the dominant peak of the first $h_{1ref}(k)$. Time delays for later sequences are estimated using respective $h_Z(k)$, so that their

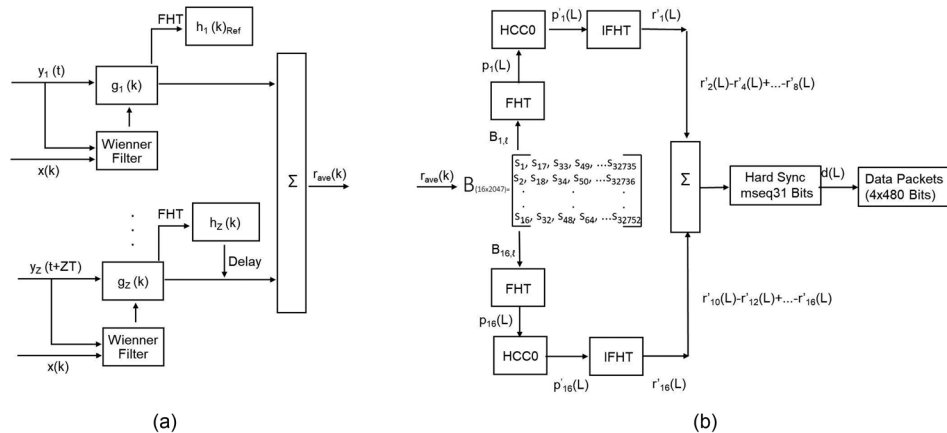


Fig. 1. (a) Diagram of channel equalization, soft synchronization, and coherent averaging of Z low SNR signals. (b) Diagram of FHT $r_{ave}(k)$, interference removal (HCC0), inverse FHT, summation, hard synchronization, and message retrieval.

strongest peaks are coincident to the reference. After alignment, coherent averaging of Z low power signals $g_Z(k)$ plus noise provides a higher SNR bitstream $r_{ave}(k)$ [Fig. 1(a)].

2.3 Interference cancellation with HCC0

The averaged bitstream $r_{ave}(k)$ is decomposed to form $B_{(16 \times 2047)}$ [Fig. 1(b)]. Synchronous sampling $r_{ave}(k)$, the first row of B , is filled by the first sample of each bit. The second row starts with the second sample, and so on. The rearrangement in matrix B shows that odd rows have samples close to zero and even rows fluctuate in amplitude but reverses the pilot phase in 180° , where $B(2, l) \simeq -B(4, l) \simeq B(6, l) \simeq \dots \simeq -B(16, l)$ for $l = 1 \dots L$. As in Sec. 2.2, an FHT is used for $r_{ave}(k)$ pulse compression [Fig. 2(a)]. Decomposing the resulting matrix FHT $_{(16 \times L)}$, for $i = 1 \dots 16$, one can observe that each baseband sequence $p_i(L)$ contains part of the pilot energy [Fig. 2(b)]. Thus, a simple cancellation of the pilot interference to the message is performed by HCC0,^{4,8,9} which zeroes out samples $q_i(l)$ having amplitudes higher than a threshold (η). In practice, the coordinate zeroing threshold is adjusted to eliminate most strong arrivals. As shown in Fig. 2(b), just a few samples are removed from each subset $p_i(L)$, resulting in $p'_i(L)$. However, the tradeoff between the number of zeroed samples and BER is not defined, depending on the channel multipath structure and noise level. To decompress the original message free from most interference, the 16 baseband $p'_i(L)$ are rearranged and an inverse fast Hadamard transform (IFHT)^{4,7,8} is used.

2.4 Hard synchronization and message retrieval

From all 16 rows in IFHT $_{(16 \times L)}$, only eight are summed up to create a single 2047-bit sequence containing the message [Eq. (2)]

$$r'_\Sigma(L) = r'_1 + r'_2, \tag{2}$$

where $r'_1 = \sum r(i, L)$ for $i = 2, 6, \dots, 14$ and $r'_2 = \sum r(j, L)$, for $j = 4, 8, \dots, 16$. As shown in Sec. 2.3, odd rows do not contribute to the summation and a change in sign of r_2 means that these sequences are 180° phase reversed compared to r_1 . Using $r'_\Sigma(L)$, hard synchronization is done using cross-correlation peaks from FHT of mseq31 which precedes data packets. After synchronization, receiver retrieves the four 480-bit data packets.

3. Shallow water LPD experiment

As proof of concept, a shallow water experiment was performed in the bay of Arraial do Cabo/ Brazil from November 28 to 29, 2018. A single directional acoustic source and a hydrophone were both assembled in fixed tripods, approximately 1 m above the bottom, in a 4 and 10 m deep water column. The bathymetry changed along the 600 m range. The source was wired to shore where the transmission system modulated data on a carrier central frequency (f_c) of 7.5 kHz (BW: 3 kHz). The data acquisition system has a sampling rate of 100 kHz and a resolution of 16 bits, but signals were downsampled to 30 kHz, 4 times f_c , before processing. The quantization noise level of 96 dB is reached at approximately 40 kHz, from which the noise power becomes constant (white). Since our system operates in the band 6–9 kHz, the received signals were predominantly perturbed by ocean noise. Mainly caused by the proximity to the city's harbor, the high broadband noise levels created undesired interference. Thus, to evaluate the performance in different scenarios, the experiment lasted 21 h with data transmissions occurring once every 30 min. Each transmission consisted of two distinct low power level blocks. In each block, to explore channel temporal diversity, the same bitstream was repeated continuously for 87 s (79 sequences), with no guard time between them. Furthermore, the four data packets in each bitstream had the same content.

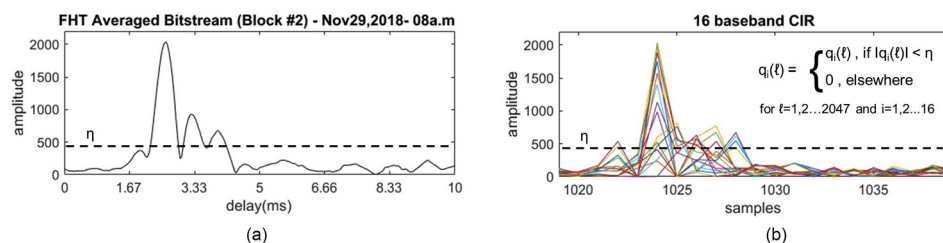


Fig. 2. (Color online) (a) Based on data from block #2 (Nov29,2018-08a.m), a FHT of averaged bitstream $r_{ave}(k)$ estimated the channel delay spread. The dashed line represents the threshold for removal of the pilot interference using HCC0. (b) Decomposition of (a) in 16 baseband CIR $p_i(L)$.

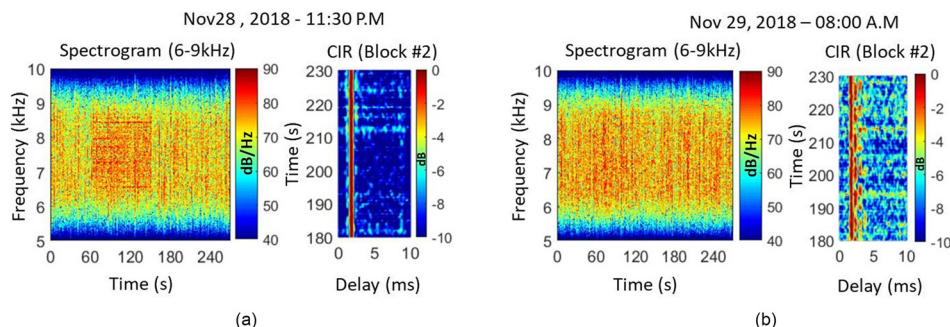


Fig. 3. (Color online) (a/b) Left: In band spectrograms from transmissions recorded on November 28, 2018 at 11:30 p.m. and November 29, 2018 at 08:00 a.m. show block # 1 (SNR: -1.4 and -5.9 dB) from 72 to 159 s and block #2 (SNR: -8.1 and -13.2 dB) from 174 to 261 s; Right: CIR estimated using FHT of bitstreams from block #2 (180 to 230 s).

Figure 3 presents an in-band spectrogram (6–9 kHz) and the CIR estimated from data recorded on November 28, 2018 at 11:30 p.m. and November 29, 2018 at 08:00 a.m. Covert communications assume that the transmitted signals are much weaker than the background noise (SNR < -8 dB within the signal band at the receiver)³ and that the unknown listener does not have a prior knowledge of the transmitted signal. Therefore, LPD signals are not expected to appear in spectrograms, a commonly used energy detectors based on an increase of SNR as a function of time and frequency.⁴ At the beginning of the experiment, the source power was set to make block #1 minimally visible (SNR: -1.4 dB) from 72 to 159 s and block #2 undetectable (SNR: -8.1 dB) from 174 to 261 s [Fig. 3(a), left]. But as the channel noise levels varied during the experiment, there were time periods where both blocks were not observed. In Fig. 3b (left), the SNR of block #1 and #2 are -5.9 and -13.2 dB.

Figures 3 also expresses the CIR variability in time estimated using bitstreams from block #2 received between 180 and 230 s. Figure 3(a) (right) shows a low noise level and light multipath environment where the direct arrivals are dominant. On the other hand, Fig. 3(b) (right) presents higher noise, stronger fading but a still short and stable multipath of approximately 2 ms. As each chip/symbol has a duration of 0.58 ms, shorter than the multipath spread, intersymbol interference degraded performance.

4. Experimental results

The received signals were contaminated with impulsive background noise. Thus, the in-band SNR (dB) was estimated according to Eq. (3),

$$SNR = 10 \log_{10} \left(\frac{S - N}{N} \right), \quad (3)$$

where S is the mean of the signal plus noise power of Z sequences; N is the mean of the noise power of a sequence of the same length of S, estimated from the period preceding the block #1.

In this work, synchronization was a major concern. Superimposing 40 CIR $h_z(k)$ estimated from data recorded in November 29, 2018 at 08:00 a.m., as shown in Fig. 3, and time gating around the dominant arrivals (200 samples or 6.7 ms), one can observe that the strongest arrivals of each sequence are not coincident [Fig. 4(a), left]. Thus, soft synchronization of CIR $h_z(k)$, using the CIR

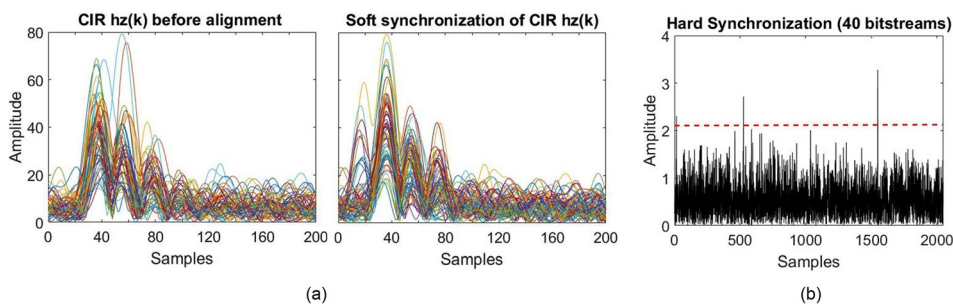


Fig. 4. (Color online) (a) Left: The first 40 CIR $h_z(k)$ before alignment. Right: Soft synchronization of $h_z(k)$ in the left, using the $h_{1ref}(k)$ as the reference. (b) Hard synchronization of the averaged bitstream composed of sequences in (a) shows the first, second, and fourth synchronization peaks crossing the threshold (dashed line). Signals from block #2 recorded on November 29, 2018 at 08:00 a.m. (SNR: -12.7 dB, BER: 3.3%).

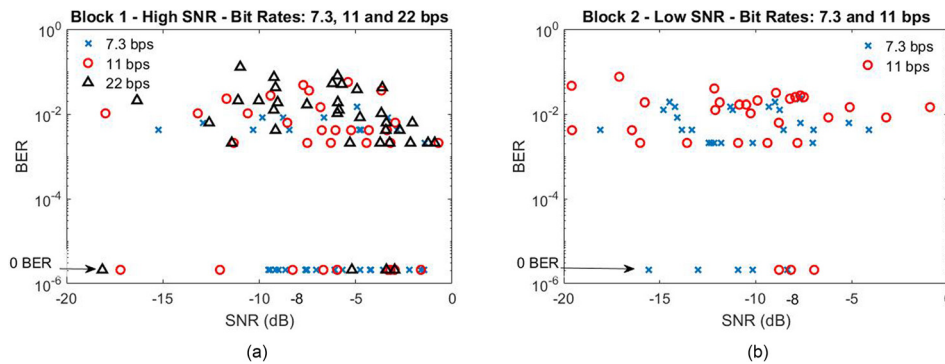


Fig. 5. (Color online) (a) Block #1—BER and SNR fluctuate during the experiment. LPD benchmark: SNR < −8 dB. Bit rates: 7.3, 11, and 22 bps. (b) Same graph as (a), for block #2. Bit rates: 7.3 and 11 bps.

$h_{1ref}(k)$ as the reference, must be performed before averaging to mitigate interference [Fig. 4(a), right]. Using the averaged bitstream $r_{ave}(k)$, the hard synchronization was performed using a mseq31 replica. Figure 4(b) shows the first, second and fourth synchronization peaks (samples: 14, 525, and 1547), crossing the detection threshold (dashed line). As the SNR was −12.7 dB, the third packet (sample: 1036) was not detected degrading the result (BER: 3.3%).

The proposed system showed stability in this time-varying channel, dealing with both variable noise levels, multipath, and fading. Doppler is generally a problem, in particular with low SNR signals. However, as the source and receiver were maintained steady in the water, both soft and hard synchronizations were performed using a zero Doppler mseq2047 and mseq31 replicas. To increase the processing gain and to implement error correction, the method performed long coherent averaging of received sequences which reduced the data rate. Figure 5 shows BER and SNR fluctuating in time, for three data rates. The bitstreams of block #1 were averaged during 21.8, 43.6, and 65.4 s (20, 40, and 60 sequences). Therefore, the data rate was 22.1, 11, and 7.3 bps, respectively [Fig. 5(a)]. Also, the need for averaging is related to received power level. Thus, just the longer averaging times were considered for the noisier block #2: 43.6 and 65.4 s for a data rate of 11 and 7.3 bps [Fig. 5(b)].

During most of the experiment, the in-band SNR of block #1 varied between 0 and −8 dB while the SNR of low power block #2 remained below −8 dB, the arbitrary threshold for covert communications.³ In both conditions, for chosen data rates, the method was able to provide BER lower than 10^{-2} in most transmissions, including several error-free messages. But Fig. 5(a) presents better BER compared to Fig. 5(b) because of the higher SNR and longer averaging times. The gaps in Fig. 5(b) were caused by synchronization problems due to an increase in the channel noise levels and degradation in the propagation conditions. No analysis about optimality was performed.

5. Conclusions

The development of LPD underwater acoustic communication methods has been encouraged in recent years. This paper presents a new approach and verifies its suitability for LPD purposes. Computationally simple, the method performs superimposed training and takes advantage of an FHT optimization for channel estimation and synchronization. The method explores the channel temporal diversity to increase the SNR, coherent averaging the received signals. Removal of intentional interference using HCC0 and an inverse FHT to decompress the message energy permits the data retrieval. A shallow water experiment presented encouraging results. Despite the low bit rate for long averaging times, the proposed approach achieved $BER < 10^{-2}$ for $SNR < -8$ dB for several received signals. Furthermore, the algorithm uses long orthogonal training codes which can permit multiple users to access the channel, minimizing mutual interference. Moreover, future work will extend the method for moving platforms where Doppler is expected, to implement error correction codes based on Hadamard matrices and a receiver array, exploring both channel temporal and spatial diversity.

Acknowledgments

This work was funded by the Postgraduate Study Abroad Program of the Brazilian Navy, Grant Nos. Port. 301/MB/2014 and 227/MB/2019, and by the U.S. Office of Naval Research (ONR Code 32). The authors are thankful to the Brazilian Navy Institute of Sea Studies Admiral Paulo Moreira (IEAPM) for the support during the experiments at sea. Comments and discussions with our colleagues from LarSys, IEAPM, and RSMAS are greatly appreciated.

References and links

- ¹R. Diamant and L. Lampe, “Low probability of detection for underwater acoustic communication: A review,” *IEEE Access* **6**(3), 19099–19112 (2018).
- ²T. C. Yang and W. Yang, “Low probability of detection underwater acoustic communications using direct-sequence spread spectrum,” *J. Acoust. Soc. Am.* **124**(1), 3632–3647 (2008).
- ³T. C. Yang and W. Yang, “Performance analysis of direct-sequence spread-spectrum underwater acoustic communications with low signal-to-noise-ratio input signals,” *J. Acoust. Soc. Am.* **123**(2), 842–855 (2008).
- ⁴T. C. Yang and W. Yang, “Interference suppression for code-division multiple-access communications in an underwater acoustic channel,” *J. Acoust. Soc. Am.* **126**(7), 220–228 (2009).
- ⁵P. Hoeher and F. Tufvesson, “Channel estimation with superimposed pilot sequence,” in *Global Telecommunications Conference GLOBECOM’99*, Rio de Janeiro, Brazil (1999), Vol. 4, pp. 2162–2166.
- ⁶W. K. Pratt, “Generalized wiener filtering computation techniques,” *IEEE Trans. Comput.* **C-21**(7), 636–641 (1972).
- ⁷A. Lempel and M. Cohn, “On fast m-sequence transform,” *IEEE Trans. Inf. Theory* **23**(1), 135–137 (1977).
- ⁸H. S. Chang, “Detection of weak, broadband signals under doppler-scaled, multipath propagation,” Ph.D. dissertation, University of Michigan, Ann Arbor, MI, 1992.
- ⁹H. DeFerrari and A. Rodgers, “Eliminating clutter by coordinate zeroing,” *J. Acoust. Soc. Am.* **117**(4), 2494 (2005).